Interacting multiple model-based human motion prediction for motion planning of companion robots*

Donghan Lee[1], Chang Liu[2] and J. Karl Hedrick[3]

***Abstract*— Motion planning of human-companion robots is a challenging problem and its solution has numerous applications. This paper proposes a motion planning method for human-companion robots to accompany humans in a socially desirable manner, which takes into account the safety, comfortableness and naturalness requirements. A unified Interacting Multiple Model (IMM) framework is developed to estimate human motion states from noisy sensor data and predict human positions in a finite horizon. The robot motion planning is formulated as a model predictive control problem to generate socially desirable motion behavior based on the predicted human positions. The effectiveness of the proposed motion planning method in facilitating the socially desirable companion behavior is evaluated through simulations and the advantage of IMM framework for human motion estimation and prediction compared to traditional single-model approaches has been demonstrated.**

I. INTRODUCTION

The application of autonomous robots for search-and-rescue (SAR) missions have received considerable attentions in last decades [**?**], [**?**], [**?**]. One particular interesting scenario is allowing autonomous robots to accompany humans during the SAR. Robot companions can follow and assist humans in carrying heavy apparatus, exploring dangerous areas or detecting signals of survivors.

Socially desirable companion behavior necessitates several requirements to be satisfied, including safety, comfort, naturalness and sociability [1]. Among these requirements, safety serves as the fundamental guideline, requiring that robots avoid collision with accompanied humans under all circumstances [2]–[4]. Comfort composes a social requirement on the robot behavior, which requires robots to pose little annoyance and stress for the accompanied humans [1]. It is mainly formulated regarding the distance that a robot needs to keep from people. For example, Hall [5] proposed the concept of "Proxemics" to denote the virtual zone around a person that other people should avoiding entering in order to prevent the discomfort the person may feel. Barnaud et al. [6] investigated the proxemics models in the context of human-aware robot navigation by investigating a classic corridor-crossing experiment. This work provides a tool for designing parameters of the proxmics model that can be used for robot motion planning in the environment with human existence. Naturalness and sociability reflect the requirements on (**TODO:** finish this sentence).

(**TODO:** move the following sentence to the method review section) By incorporating these requirements into account, researchers have developed several human-companion robots. In [**?**], a generalized framework for representing social conventions as components of a constrained optimization problem was presented and it was used for path planning and navigation.

Cosgun et al. [7] develops a robot for telepresence usage, which uses the laser scanner to track human movement and predicts human path by extrapolating based on the estimated human position and speed, assuming a constant velocity human motion model. The robot utilizes the depth-limited breadth-first search approach to find the waypoints around the predicted human positions so that the robot can always face the accompanied human with a similar velocity as the human. Hoeller et al. [2] presents a local path planning approach for the companion robot to stay in proximity to the target person and simultaneously prevent colliding with any passers-by. The probabilistic roadmaps is used to plan collision-free paths to a given target location, chosen based on the predicted adjacent humans' positions. A laser-based people tracking technique is used to estimate the motions of humans and a potential field method is applied for predicting the humans future trajectories.

To generate socially desirable motion behavior, accurate human motion estimation and prediction is necessary, which can be then utilized for robot motion planning. To be specific, a robot needs to estimate motion states of the accompanied human in real time based on measurements from equipments such as GPS sensors or cameras and then predict human future trajectory. There exist several widely-adopted estimation methods, such as the Kalman filter [**?**], which provides the minimum mean square error estimation of states for linear systems with Gaussian noise. (**TODO:** find references for its application to motion estimation and prediction) The Extended Kalman filter (EKF) and Unscented Kalman filter (UKF) [**?**], which are extensions of the KF for nonlinear systems, have also been applied for motion estimation and prediction [**?**]. EKF can be obtained by applying the KF to the first-order Taylor expansion of nonlinear systems while UKF uses a deterministic sampling technique, called the Unscented Transform, to perform a stochastic linearization through the use of a weighted statistical linear regression process [8]. (**TODO:** if the references for motion estimation

*This work was not supported by any organization

[1]Donghan Lee with the Vehicle Dynamics & Control Lab, Department of Mechanical Engineering, University of California at Berkeley, California 94720, USA donghan.lee@berkeley.edu

[2]Chang Liu with the Vehicle Dynamics & Control Lab, Department of Mechanical Engineering, University of California at Berkeley, California 94720, USA changliu@berkeley.edu

[3]J. Karl Hedrick is with Faculty of Mechanical Engineering, University of California at Berkeley, California 94720, USA khedrick@berkeley.edu

and prediction using xKF methods can be found, then remove the following part.) Based on the estimated states, extrapolation assuming known human motion models, such as the constant velocity and constant turn model (**TODO:** lit review), can be applied for predicting human positions in a finite horizon.

[Note:] try to merge the following sentence with the previous one.

These methods usually assumes a single motion model for estimation and prediction and have been widely applied in motion planning and localization in the field of robotics [8].

In recent years, machine learning techniques have been utilized for human motion prediction. Bennewitz et al. [9] proposed a technique for learning collections of trajectories that characterize typical motion patterns of persons Trajectories were clustered using Expectation Maximization algorithm and a hidden Markov model was then applied to predict future positions of persons based on sensory input in real time. Fulgenzi et al. [10] developed an approach for predicting trajectories of moving objects, which were supposed to move with typical patterns with some amount of uncertainty. Those patterns were represented by Gaussian processes and pre-learned based on the collected set of trajectories. A two-layer prediction that combined long-term destination inference and short-term motion prediction was proposed in [11]: the short-term prediction that refers to the one-step ahead prediction of a humans future position was achieved by a Polynomial Neural Network (PNN), which was trained offline; the long-term prediction was performed by utilizing the heading direction of a human to determine the destinations where he/she would have interest in visiting.

These approaches have achieved success in predicting human motion trajectories. However, they usually involves the collection of training data (e.g., recorded human trajectory) and are prone to be scenario specific. In fact, human motion can be well predicted using these machine learning-based prediction approaches in the scenarios where human trajectories have been collected used for training predictors. However, these predictors may fail to obtain accurate prediction in unknown environments. This drawback renders the machine learning-based methods less applicable for search and rescue missions since disaster sites are rarely similar to the known ones and therefore robots need to work in unfamiliar environments.

Human motion usually involves different identified motion models, such as straight-line movement, making turns and change of speed. Therefore, a model-based approach would be promising to generate accurate prediction results. In this work, we employ the Interacting Multiple Model (IMM) approach for human motion estimation and prediction. IMM is a model-based estimation framework that takes into several system models into account and dynamically adjusts the mode probabilities. To deal with the nonlinear dynamics of the human motion (such as making turns), UKF is applied to each model in the IMM framework, resulting in the so-called IMM-UKF approach. Such approach can achieve higher accuracy compared to traditional estimation and prediction methods that utilize a single motion model. Additionally, no training is needed and thus scenario-independent, which is advantageous over machine learning methods for search and rescue missions. Utilizing the predicted human trajectory, a model predictive control (MPC)-based motion planner is developed for the companion robot to autonomously accompany the target person in a socially desirable manner, which takes into consideration the safety and comfort requirements. The main contribution of this paper is ... (**TODO:** need to fill this paragraph).

The remainder of this paper is organized as follows: first, the problem of motion planning for a human-companion robot is formulated for the SAR mission; second, the IMM-UKF estimation and prediction method is described, followed by the MPC planner; next, simulation setup and results on evaluating the proposed approach are presented; lastly, concluding remarks and ideas of future work are presented.

II. PROBLEM FORMULATION

Considering the SAR scenario (Fig. 1a) in which a human first responder needs to deliver medical treatment to several destinations that contain injured people. A companion robot that carries medical apparatus will accompany the human and sequentially move to these destinations. The human follows the trajectory that is shown in Fig. 1d. Such trajectory covers several typical human motion patterns, including straight-line movement, motion following curved paths and making sharp turns. The robot has no knowledge about the positions of human destinations, nor the pre-designed human trajectory. However, it can measure human positions in real time from the GPS sensor that the human carries. Several obstacles exist in the field, including five stationary ones and two moving ones, representing unmovable obstructions, such as buildings or plants, and mobile objects, such as pedestrians or vehicles, respectively. Figs. 1b and 1c show that the moving obstacles start to act. The positions of stationary obstacles are known to both the human and the companion robot while the moving obstacles are measured using same measurement tool for tracking the human rescuer. When accompanying the human, the robot should satisfy the aforementioned safety and comfort requirements. To be specific, a circular safety zone" with radius d_s (**??**) is defined around the target person, indicating the area that the robot should avoid entering. Stepping into the "safety zone" is considered as unsafe behavior and thus should be avoided. The comfort requirement consists of two parts: the robot needs to maintain a comfortable distance d_c from the human, as investigated in [5], and also keep similar speed with the human, as shown in [**?**].

III. METHODS

A. Human Motion Estimation

The Interacting Multiple Model (IMM) approach are applied for estimating the human motion from the noisy sensor data. It utilizes a bank of r number of filters, each (designed to model) (**TODO:** corresponding to) a different dynamics.

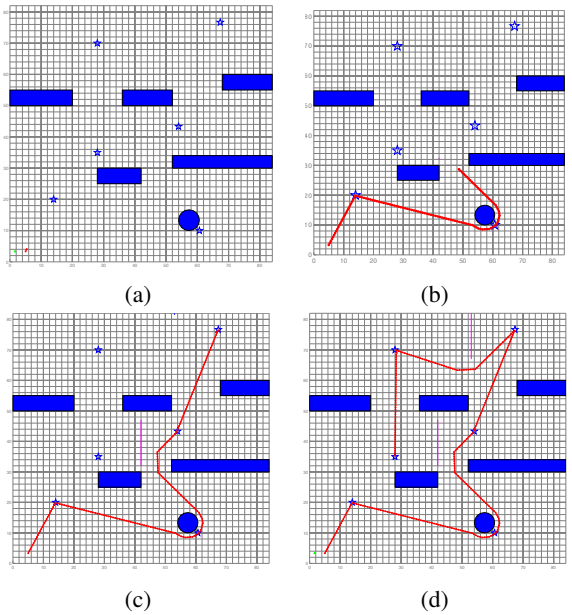

Fig. 1: A search-and-rescue scenario for the companion robot to accompany a human. (a) The initial state of the scenario. The red circle and the green triangle represent the human rescuer and the robot companion, respectively. Stars denote human destinations and the blue rectangles stand for static obstacles. (b) The 1st moving obstacle starts moving. (c) The 2nd moving obstacle starts moving. (d) The full human trajectory.

[Note:] dh: change moving obstacles' color to make it more obvious; add arrows to them to show the direction.

State estimate at time k is computed as a weighted sum of estimates from each filter, as shown in the following formula:

[Note:] mu_i or mu_j?

$$\hat{x}(k|k) = \sum_{j=1}^{r} \mu_j(k)\hat{x}^j(k|k)$$

where r denotes the number of models; $\hat{x}^j(k|k)$ represents the state estimate from the j^{th} filter; $\mu_j(k)$ stands for the mode probability and is computed as follows:

$$\mu_j(k) = \frac{1}{c}\sum_{i=1}^{r} L_{ij}(k)p_{ij}\mu_j(k-1)$$

where c denotes the normalizing factor; $L_{ij}(k)$ stands for the likelihood function and p_{ij} represents the mode transition probability from the i^{th} to the j^{th} model. Each filter uses the mixed initial state estimate and covariance from different combination of the previous model. Readers interested in the details of the IMM approach can refer to [**?**].

In this work, two different dynamic models are used in the IMM framework: one is the coordinated turn motion model, reflecting the action of making turns or moving along a curved path, and the other is the uniform motion model, representing the straight-line movement. The equation of motion for the both the coordinated turn motion and uniform motion model becomes the following (**TODO:** is this the equation of turn motion model only?)

$$x^{h,1}(k+1) = f(x^{h,1}(k)) + Gw(k) \tag{1a}$$

$$f(x^{h,1}(k)) = \begin{bmatrix} p_1^h + \frac{\sin(\omega^h T)}{\omega^h}v_1^h - \frac{1-\cos(\omega^h T)}{\omega^h}v_2^h \\ \cos(\omega^h T)v_1^h - \sin(\omega^h T)v_2^h \\ p_2^h + \frac{1-\cos(\omega^h T)}{\omega^h}v_1^h + \frac{\sin(\omega^h T)}{\omega^h}v_2^h \\ \sin(\omega^h T)v_1^h + \cos(\omega^h T)v_2^h \\ \omega^h \end{bmatrix} \tag{1b}$$

$$G = \begin{bmatrix} \frac{T^2}{2} & 0 & 0 \\ T & 0 & 0 \\ 0 & \frac{T^2}{2} & 0 \\ 0 & T & 0 \\ 0 & 0 & 1 \end{bmatrix} \tag{1c}$$

$$w \sim \mathcal{N}(0, Q) \tag{1d}$$

where $x^h(k)$ represents the human motion state including five elements : $p_1^h, v_1^h, p_2^h, v_2^h, \omega^h$, where p_1^h, p_2^h denote the longitudinal and lateral position of the human, v_1^h, v_2^h the corresponding velocity and ω^h the turn rate of the human; $w(k)$ represents process noise; T represents the sampling time; Q is the covariance matrix of the process noise.

The uniform motion model is essentially a special case of the coordinated turn motion model with the turn rate ω being fixed to zero. It seems that only considering the coordinated turn motion model suffices to estimate human motion states, in addition to the benefits of reduced computations by using the single model. However, including two models are necessary since this allows the estimator for fast detection of change of motions.

[Note:] May need to make the point clearer in the following sentences.

The decision is a bit clearer in linear case since the turn rate is fixed in linear dynamic models. With a single nonlinear model, it is possible to provide accurate state estimates. However, it is common to include one uniform motion model and one coordinated turn motion model for quick motion-change detection. Since human motion usually involves different motions in the real world, the ability to quickly detect the change of the motion is one of the important properties for the estimation and prediction.

(**TODO:** may present the uniform motion model before commenting on it) The equation of the uniform motion model is shown as follows:

$$\dot{x}^{h,2}(k+1) = Ax^{h,2}(k) + Bw(k) \tag{2a}$$

$$A = \begin{bmatrix} 1 & T & 0 & 0 & 0 \\ 0 & 1 & 0 & 0 & 0 \\ 0 & 0 & 1 & T & 0 \\ 0 & 0 & 0 & 1 & 0 \\ 0 & 0 & 0 & 0 & 0 \end{bmatrix}, \; B = \begin{bmatrix} \frac{T^2}{2} & 0 & 0 \\ T & 0 & 0 \\ 0 & \frac{T^2}{2} & 0 \\ 0 & T & 0 \\ 0 & 0 & 1 \end{bmatrix} \tag{2b}$$

The observation equation is represented as :

$$y^h(k) = Cx^h(k) + v(k) \tag{3a}$$

where $y^h(k)$ denotes the observed human state at the time step k; $v(k)$ stands for measurement noise.

By using GPS sensors or cameras, the human positions can be measured. Therefore, the parameters in observation model Eq. (3a) is defined as:

$$C = \begin{bmatrix} 1 & 0 & 0 & 0 & 0 \\ 0 & 0 & 1 & 0 & 0 \end{bmatrix}, \tag{4a}$$

$$v \sim \mathcal{N}(0, V) \tag{4b}$$

where V is the convariance matrix of the measurement noise. The above two models are utilized for human motion state estimation, in combination with the Unscented Kalman Filter.

B. Unscented Kalman Filter

The Unscented Kalman Filter (UKF) is applied to each model that are used in IMM framework for estimating human states. It is an effective state estimation technique for nonlinear systems by implementing the Unscented Transformation (UT) that calculates the statistics of a random vector that undergoes a nonlinear transformation [**?**]. To be specific, given an arbitrary nonlinear dynamic model $z = f(x)$ and as L-dimensional Gaussian Random Vector (GRV) x with mean $\hat{x}$ and covariance P_x(**TODO:** how to choose the mean and Covariance), the statistics of z can be approximated by using $2L + 1$ discrete sample points $\{\chi^{(i)}\}_{i=0}^{2L} = \{\hat{x} \text{ and } \hat{x} \pm \sigma_j, j = 1, ..., L\}$, where σ_i is the i^{th} column of the matrix $\sqrt{(L+\lambda)P_x}$. λ is a scaling parameter, as defined below:

$$\lambda = \alpha^2(L + \kappa) - L \tag{5a}$$

$$W_0^{(m)} = \frac{\lambda}{L+\lambda} \tag{5b}$$

$$W_0^{(c)} = \frac{\lambda}{L+\lambda} + 1 - \alpha^2 + \beta \tag{5c}$$

$$W_i^{(m)} = W_i^{(c)} = \frac{1}{L+\lambda}, \quad i = 1, ..., 2L \tag{5d}$$

where α determines the spread of sigma points(**TODO:** May need to give the definition here) about the mean $\hat{x}$; κ is a secondary scaling parameter; β is used to incorporate prior knowledge of the distribution. (**TODO:** move this to the simulation section)(our simulation uses $L = 5, \alpha = 0.001, \kappa = 0, \beta = 2$)

Once the discrete sample points $\{\chi^{(i)}\}_{i=0}^{2L}$, called *sigma points*, have been generated, each point is passed through the nonlinear function $z = f(x)$, i.e. each column of the sigma points is propagated through the non-linearity, as in $\zeta = f(\chi), i = 0, ..., 2L$. The mean $\hat{z}$ and the covariance P_z are approximated as $\hat{z} \simeq \Sigma_{i=0}^{2L} W_i^{(m)} \zeta^{(i)}$ and $P_z \simeq \Sigma_{i=0}^{2L} W_i^{(c)} (\zeta^{(i)} - \hat{z})(\zeta^{(i)} - \hat{z})^\intercal$, (**TODO:** some typo?)are calculated as given in above equations of the weights and parameters [**?**]. Readers can refer to [**?**] for more details of the UKF algorithm.

C. Human Motion Prediction

The estimated human motion states and the mode probabilities are utilized for predicting human future states. To be specific, using the uniform motion model and the turn motion model, human positions for each model can be extrapolated and then combined based on the mode probabilities to obtain the predicted positions. Let $\hat{x}^{h,j}(k|k)$ and $\tilde{x}^{h,j}(k+i|k)$ represent the estimated and predicted human states associated with the j^{th} model at time k and $k+i\,(i \geq 0)$, respectively, based on the observations up to time k. The prediction procedure works as follows:

[Note:] what's the difference between two sides of Eqn. (6c)?

$$\tilde{x}^h(k+l+1|k) = \sum_{j=1}^{r} \mu_j \tilde{x}^{h,j}(k+l+1|k) \tag{6a}$$

$$l = 0, \ldots, N-1 \tag{6b}$$

$$\tilde{x}^{h,j}(k+l+1|k) = \hat{x}^{h,j}(k+l+1|k) \quad j = 1, \ldots, r \tag{6c}$$

$$= \Sigma_{i=0}^{2L} W_i^{(m)} \chi_{k+l+1|k}^{(i)} \tag{6d}$$

$$\chi_{k+l+1|k}^{(i)} = f(\chi_{k+l|k}^{(i)}) \quad i = 0, \ldots, 2L \tag{6e}$$

where N denotes the prediction horizon; r represents the number of models; L is the dimension of $x^{h,j}$. For the purpose of simplicity, we define $p^h(k) = \begin{bmatrix} p_1^h(k) \\ p_2^h(k) \end{bmatrix}$ and $v^h(k) = \left\| \begin{bmatrix} v_1^h(k) \\ v_2^h(k) \end{bmatrix} \right\|_2$ to represent the position vector and the speed of the human at time k, respectively. Notations for the estimated and predicted position vector and speed can be defined as $\hat{p}^h(k|k), \tilde{p}^h(k+i|k), \hat{v}^h(k|k), \tilde{v}^h(k+i|k)$, respectively.

D. Robot Path Planning

The model predictive control (MPC) approach i utilized for robot motion planning. MPC provides an effective framework for incorporating the safety and comfort requirements into the planning procedure. It iteratively solves a finite-horizon constrained optimal control problem. After obtaining the optimal control inputs over the planning horizon, it implements the first input and then computes for a new set of control inputs, starting from the updated state. Let $(p^r(k), v^r(k), \theta^r(k))$ denote the robot state at time k, representing the position, speed and heading angle, respectively. The control input consists of the acceleration $a^r(k)$ and the angular velocity $\omega^r(k)$. The optimal control inputs are obtained by solving a nonlinear programming problem that incorporates the kinematics of the robot and the safety and

comfort requirements:

$$\min_{\mathbf{A}_k,\mathbf{\Theta}_k} \quad \sum_{i=1}^{N} q_1 \left| \left\| \bar{p}^r(k+i|k) - \tilde{p}^h(k+i|k) \right\|_2^2 - d_c^2 \right| + q_2 \left| \bar{v}^r(k+i|k) - \tilde{v}^h(k+i|k) \right|^2 \tag{7a}$$

subject to
$$\bar{p}^r(k+i+1|k) = \bar{p}^r(k+i|k) + \bar{v}^r(k+i|k) \begin{bmatrix} \cos\bar{\theta}(k+i|k) \\ \sin\bar{\theta}(k+i|k) \end{bmatrix} T \tag{7b}$$

$$\bar{v}^r(k+i+1|k) = \bar{v}^r(k+i|k) + \bar{a}(k+i|k)T \tag{7c}$$

$$\bar{\theta}^r(k+i+1|k) = \bar{\theta}^r(k+i|k) + \bar{w}(k+i|k)T \tag{7d}$$

$$a_{lb} \leq \bar{a^r}(k+i|k) \leq a_{ub} \tag{7e}$$

$$w_{lb} \leq \bar{\omega^r}(k+i|k) \leq w_{ub} \tag{7f}$$

$$||\bar{p}^r(k+i+1|k) - \tilde{p}^h(k+i+1|k)||_2 \geq d_s \tag{7g}$$

$$||\bar{p}^r(k+i+1|k) - \tilde{p}_{l_m}^{obs_m}(k+i+1|k)||_2 \geq d_s \tag{7h}$$

$$h_{l_s}(\bar{p}^r(k+i+1|k)) \geq 0 \tag{7i}$$

$$h_{l_s}(\lambda\bar{p}^r(k+i|k) + (1-\lambda)\bar{p}^r(k+i+1|k)) \geq 0 \tag{7j}$$

$$\forall l = 1, \ldots, m,\ 0 \leq \lambda \leq 1$$

$$\bar{p}^r(k|k) = p^r(k) \tag{7k}$$

$$\bar{v}^r(k|k) = v^r(k) \tag{7l}$$

$$\bar{\theta}^r(k|k) = \theta^r(k) \tag{7m}$$

where $\bar{p}^r(k+i|k)$, $\bar{v}^r(k+i|k)$ and $\bar{\theta}(k+i|k)$, $0 \leq i \leq N$ represent the planned position, speed and heading angle at time $k+i$, respectively; N is the prediction horizon. n_s is the number of static obstacles and $p_{l_s}^{obs_s}$ denotes the position of the l_s^{th} obstacle; n_m stands for the number of moving obstacles and $p_{l_m}^{obs_m}$ and $r_{l_m}^{obs_m}$ denote the position and the radius of the l_m^{th} obstacle; $(\mathbf{A}_k, \mathbf{\Theta}_k)$ stand for the set of optimal acceleration and angular velocity in the prediction horizon $[k, k+N-1]$, obtained by solving the above optimization problem at time k.

The objective function Eq. (7a) consists of two terms: the first one stands for the difference between the squared human-robot distances and the squared comfort distance; the second one represents the speed difference between the robot and the human. This reflects the comfort requirement that the robot maintain the comfort distance from the human and keep similar pace at the same time. q_1 and q_2 denote the weights for these two terms. Eqs. (7b) to (7f) represent the roboot's discrete-time kinematic model with limited acceleration and angular velocity, with a_{lb}, w_{lb} being the corresponding lower bounds and a_{ub}, w_{ub} the upper bounds. The safety constraints are imposed in Eqs. (7g) to (7j). Eqs. (7g) and (7h) regulates that the robot stay at least the safety distance d_s from the human and moving obstacles in order to avoid collision. To avoid moving obstacles, the same motion prediction method described in Section III-C is applied **????** enforce the collision avoidance with static obstacles. To be specific, Rectangular obstacles are approximated by ellipsis, the details of which are described in the Appendix. Let h_{l_s} represent the analytical epxeression of the ellipse approximation of the l_s^{th} obstacle. **??** demands that each way point of the robot be kept outside of static obstacles. And **??** requires that the trajectory connecting the adjacent way points not intersect with obstacles, which eliminates the waypoints that leads the robot across obstacles. Eqs. (7k) to (7m) initializes the robots planned states based on its actual state at time k.

IV. SIMULATION RESULTS & DISCUSSION

A. Simulation setup

Simulations have been run to evaluate the proposed robot motion planning approach. One human rescuer will move sequentially to five targets in a $84m \times 82m$ field, accompanied by a robot companion. The human speed is set to be constant at $1.5m/s$. The human will follow the trajectory shown in Fig. 1d. However, this trajectory is unrevealed to the robot. The safety distance d_s is chosen as $1m$ and the comfort distance d_c as $2m$. The sampling rate of GPS sensor is $20Hz$ and the variance of sensor measurement noise is considered as $2m$. The robot's maximum acceleration and deceleration are set to be $1m/s^2$ and $-3m/s^2$ respectively and the angular velocity range is chosen to be $[-90°/s, 90°/s]$. In the IMM estimator, the process noise and the measurement noise are set to be 1.5×10^{-2} and 1.5, respectively. The prediction horizon for the human motion is chosen as $500ms$ and the robot recomputes the MPC problem every $500ms$.

B. Simulation results

We evaluate the performance of human motion estimation and prediction and the robot motion planning method, respectively.

1) Human motion estimation: The error between the estimated and the actual human position and speed at each time step are compared to evaluate the estimation accuracy. The position error vector can be formulated as:

$$\Delta_p^t(k) = p^h(k) - \hat{p}^h(k|k)$$

where $p^h(k)$ denotes the actual human position at time k.

Fig. 2 shows the position estimation error on longitudinal and lateral directions using four different estimators: Linear Kalman Filter (LKF), IMM-LKF, UKF and IMM-UKF. In the simulation, the same turn motion model in IMM-UKF is adopted for the system dynamics in UKF and the uniform motion model in IMM-LKF is also applied to the dynamic model in LKF. There are two observations in this figure. First, the responses of the nonlinear estimators such as UKF and IMM-UKF are faster than the linear estimators. Second, the IMM-based approaches show better performance in accuracy than the single-model approaches. Besided, IMM-UKF achieves the fastest response and best accuracy compared to other methods, especially when the human turns around the circular obstacle at time 50 and makes sharp turn after arriving at a destination at time 110. Fig. 3 compares the velocity estimation using four estimators. Overall, the nonlinear estimators (UKF and IMM-UKF)

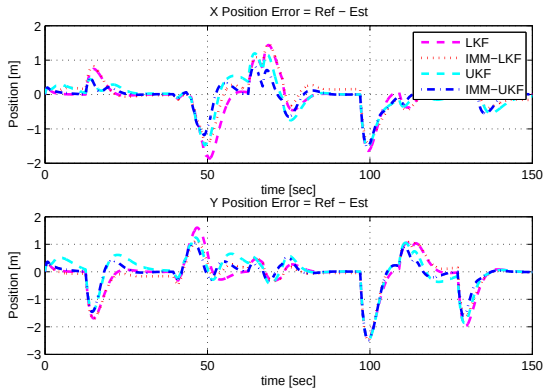

Fig. 2: Comparison of position estimation error with LKF, IMM-LKF, UKF and IMM-UKF

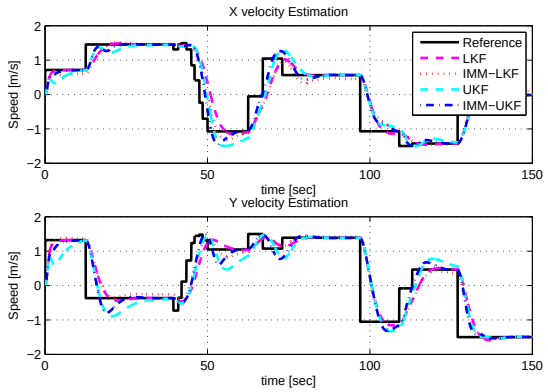

Fig. 3: Comparison of the estimated velocity using the IMM-based and the single-model approaches

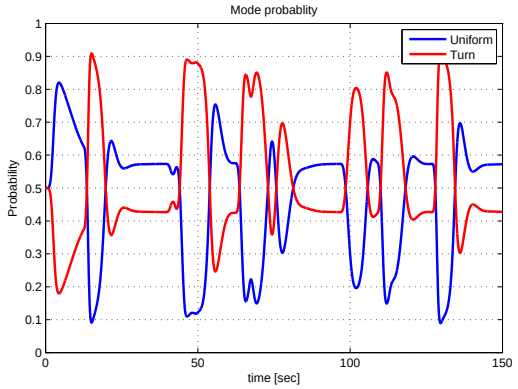

Fig. 4: Model probabilities of two models in the IMM-UKF estimator

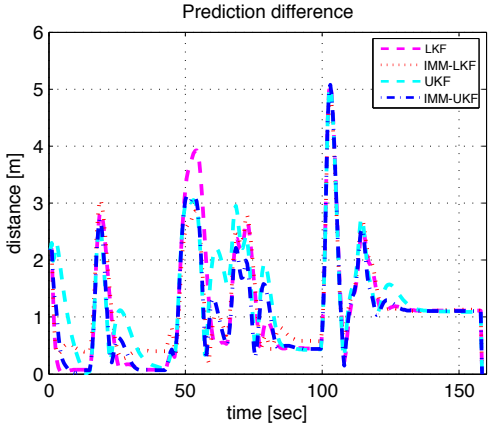

Fig. 5: Comparison of prediction error between the IMM-based and single-model approaches

show faster response compared to the linear estimators (LKF and IMM-LKF), though they have overshoots due to the fast response. It is worth noting that the overshoots of IMM-UKF are smaller than UKF while keeping the fast response at time 53 and 118 when the velocity changes abruptly. This makes sense as the UKF-IMM estimator incorporates uniform motion model that can capture the sudden velocity changes. Fig. 4 shows the mode probabilities of the uniform motion model and turn motion model in IMM-UKF over time. When the human speed changes, the mode probability of the turn motion becomes higher than that of the uniform motion. These changes illustrates the reason that IMM-based estimators achieve more accurate and faster estimation than the single-model estimator at the sharp turn and circular turn, thus demonstrating the necessity of applying IMM-UKF estimator for human tracking.

2) Human motion prediction: To evaluate the IMM-based prediction approaches, the average prediction error over the prediction horizon is computed and compared with the single-model approaches. At time k, the prediction error is defined as:

$$\Delta_p(k) = \frac{1}{N}\sum_{i=1}^{N} ||\tilde{p}^h(k+i|k) - p^h(k+i)||_2 \qquad (8)$$

Different from the IMM-based prediction approaches that extrapolate the human position by a weighted sum of the predicted positions from each model, the single-model methods only utilize the uniform motion model for prediction.

Fig. 5 shows the comparison of prediction error using two single-model approaches (LKF, UKF) and two IMM-based methods (IMM-LKF, IMM-UKF). It can be noticed that single-model approaches generate larger prediction error than IMM-based methods, especially when the human makes turns, such as at time 50. This makes sense as IMM-based method considers different dynamic models related to the human motion. Based on the simulation results, IMM-UKF outperforms the other three methods for prediction.

3) Robot motion planning: Fig. 6 shows the trajectory of the companion robot that accompanies the target person

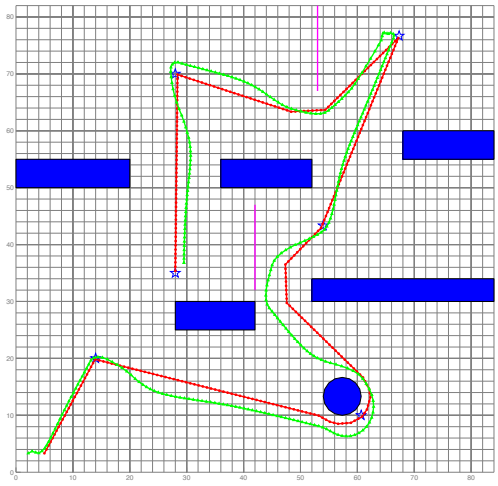

Fig. 6: A screenshot of the simulation. The red line represents the human trajectory and the green on shows the companion robot's trajectory. For most of the time, the robot follows the human from behind(**TODO:** legend uses upper)

TABLE I: human-robot distance

Method	IMM-UKF	UKF	non-prediction
Ave	1.4323	1.5890	2.6053
Std	0.9367	0.9023	0.6428

moving in the field. The trajectory is generated by the proposed MPC motion planner and using the IMM-UKF for predicting human and moving obstacles' trajectories. The performance of the motion planning is evaluated using the criterion of safety and comfort. To be specific, the distance and speed differences between the robot and the human at each time step are measured, which are defined as:

$$\Delta_d(k) = ||p^r(k) - p^h(k)||_2 - d_s \tag{9a}$$

$$\Delta_v(k) = |v^r(k) - v^h(k)| \tag{9b}$$

These quantities are illustrated as the blue line in Figs. 7 and 8.

The performance of IMM-UKF predictor for robot motion planning is evaluated by comparing with two benchmark prediction strategies, while using the same MPC planner. The first benchmark method applies a single-model predictor (UKF predictor) to the coordinate turn motion model

[Note:] Dong-han, is this correct?

and predicts human motion. The second one does not predict human motion. Instead, the robot only utilize the human's current state for one-step motion planning.

Fig. 7 compares the distances between the human and the robot using these threestrategies. Notice that the distances in the plot has been substracted by the safety distance d_s.

TABLE II: speed difference

Method	IMM-UKF	UKF	non-prediction
Ave	0.1018	0.1194	0.0189
Std	0.2588	0.2510	0.2032

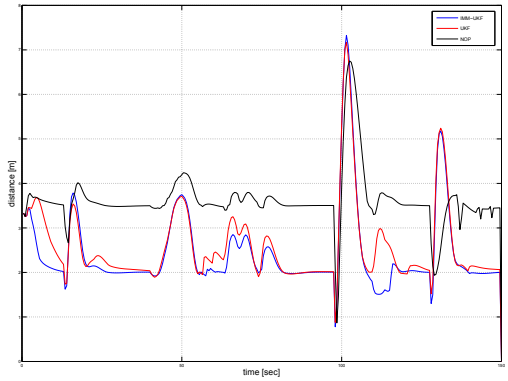

Fig. 7: Comparison of distance (substracted by the safety distance) between the human and the robot using the MPC and the reactive methods

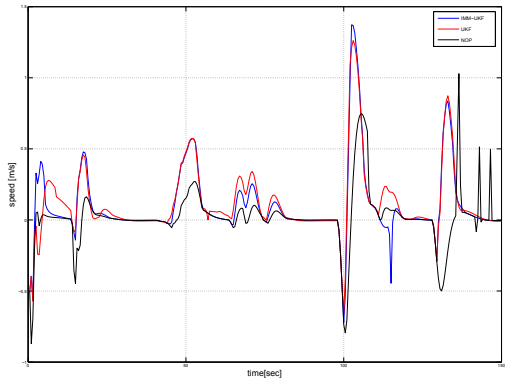

Fig. 8: Comparison of velocity difference between the human and the robot using the MPC and the reactive methods

Therefore, distance values less than zero at any time step are considered unsafe and thus undesirable. In addition, distance around $d_c - d_s$ is desired, as it implies that the robot keeps a comfortable distance d_c from the human. It can be noticed that the MPC planner has ensured the safety of the accompanied human with each of the three prediction methods. Additionally, by incorporating human motion prediction into the motion planning, the robot improves its companion performance from the non-prediction case. This can be demonstrated by Table I that the mean of human-robot distance using the prediction is much smaller than that without prediction. Additionally, the IMM-UKF predictor achieves better performance than the UKF-predictor in that the average distance is smaller but still within the comfort range using the former predictor than with the latter one.

The non-prediction method achieves smaller velocity difference than methods using predictors. This seems to imply that the non-prediction method is preferable for robot to similar pace as the human. However, such similarity using non-prediction method results in unsatisfactory following behavior, as shown in Fig. 7. In general, the simulation results show the superiority of using the multiple-model predictor (IMM-UKF predictor) for robot motion planning.

V. CONCLUSION

We have developed a model predictve control (MPC)-based motion planning approach for human-companion robots to accompany a target person in a socially desirable manner, which considers the safety and comfort of the behavior. Such companion robot can be useful for search and rescue scenarios by carrying apparatus, exploring dangerous areas and detecting survivors. The IMM-UKF approach that incorporates the uniform motion model and the coordinated turn motion models is developed for human position estimation and prediction. Such multiple-model approach captures different motion patterns, thus improving the estimation and prediction accuracy than other single-model approaches. Based on the predicted human positions, the model predictive control (MPC) approach is formulated for planning socially desirable motion trajectory. The estimation and prediction accuracy using IMM-UKF is compared with IMM-LKF and two single-model methods (LFK and UKF). Comparison results show superior accuracy and response in estimation and prediction using IMM-UKF approach, especially when the human makes circular motion or sharp turns. Moreover, the MPC planner using IMM-UKF predictor, UKF predictor and no predictor are compared. The IMM-UKF predictor improves the robot motion behavior that keeps human-robot distances around the comfort distance and similar velocity.

In the future work, we plan to investigate other motion prediction methods, such as the autoregressivemoving-average method, to compare with IMM-UKF method. Besides, enabling the robot to learn human motion model in real time is an attractive topic and may provide more accurate human motion prediction and results in better human-companion behaviors.

VI. APPENDIX

A. IMM-LKF Predictor

Similar to IMM-UKF, IMM-LKF works with two dynamic models: one is the uniform motion model; the other is the coordinated turn motion model. If the turn rate is a known constant in the coordinated turn motion model in **??**, the human estimation procedure can be modeled with the discrete time linear state space system as follows:

$$x^h(k+1) = Ax^h(k) + B_w w(k) \tag{10a}$$

$$y^h(k) = Cx^h(k) + v(k) \tag{10b}$$

where $x^h(k)$ and $y^h(k)$ represent the human motion state and the observation, respectively, at the time step k; $w(k)$ and $v(k)$ represent process noise and measurement noise, respectively. $x^h(k)$ consists of four elements: $p_1^h, v_1^h, p_2^h, v_2^h$, where p_1^h, p_2^h denote the longitudinal and lateral position of the human and v_1^h, v_2^h the corresponding velocity. We use two Linear Kalman Filters in the IMM for human tracking, each corresponding to a different dynamics model: the uniform motion model and the turn motion model. Two models differ in the A matrix and w in Eq. (10a) while sharing the same B_w. In particular, we define the matrices as follows:

$$A_U = \begin{bmatrix} 1 & T & 0 & 0 \\ 0 & 1 & 0 & 0 \\ 0 & 0 & 1 & T \\ 0 & 0 & 0 & 1 \end{bmatrix}, \tag{11a}$$

$$A_T = \begin{bmatrix} 1 & \frac{\sin(\omega T)}{\omega} & 0 & \frac{1-\cos(\omega T)}{\omega} \\ 0 & \cos(\omega T) & 0 & -\sin(\omega T) \\ 0 & \frac{1-\cos(\omega T)}{\omega} & 1 & \frac{\sin(\omega T)}{\omega} \\ 0 & \sin(\omega T) & 0 & \cos(\omega T) \end{bmatrix}, \tag{11b}$$

$$B_w = \begin{bmatrix} \frac{T^2}{2} & T & 0 & 0 \\ 0 & 0 & \frac{T^2}{2} & T \end{bmatrix}, \tag{11c}$$

$$w_U \sim \mathcal{N}(0, Q_U)\ w_T \sim \mathcal{N}(0, Q_T) \tag{11d}$$

where A_U and A_T stand for the A matrices of the uniform motion model and turn motion model, respectively; w_U and w_T denote the process noise of the uniform motion model and turn motion model, respectively; T represents the sampling time; ω represents the constant turn rate.

We assume that only the human position can be measured. Therefore, the parameters in observation model Eq. (10b) can be defined as:

$$C = \begin{bmatrix} 1 & 0 & 0 & 0 \\ 0 & 0 & 1 & 0 \end{bmatrix}, \tag{12a}$$

$$v \sim \mathcal{N}(0, V) \tag{12b}$$

Above linear state space models are used in LKF and IMM-LKF in this paper. Moreover, we set the turn rate ω to be 0.1 rad/s as a known constant, in the turn motion model in IMM-LKF.

B. Approximating Static Obstacles

Static rectangular obstacles are approximated and analytically represented as ellipses, as shown in **??**. Let l and m be the length and width of a rectangular obstacle centered at the origin. Let Section VI-B represent the ellipse that encloses the obstacle in the way that the four vertices of the rectangle lie on the boundary of the ellipse.

$$\frac{x^2}{a^2} + \frac{y^2}{b^2} = 1$$

In addition, assume that the rectangle and ellipse have the same aspect ratio, which means $\frac{l}{m} = \frac{a}{b}$, then $a = \frac{l}{\sqrt{2}}$ and $b = \frac{m}{\sqrt{2}}$.

REFERENCES

[1] T. Kruse, A. K. Pandey, R. Alami, and A. Kirsch, "Human-aware robot navigation: A survey," *Robotics and Autonomous Systems*, vol. 61, no. 12, pp. 1726–1743, 2013.

[2] F. Hoeller, D. Schulz, M. Moors, and F. E. Schneider, "Accompanying persons with a mobile robot using motion prediction and probabilistic roadmaps," in *Intelligent Robots and Systems, 2007. IROS 2007. IEEE/RSJ International Conference on*, pp. 1260–1265, IEEE, 2007.

[3] D. Fox, W. Burgard, S. Thrun, *et al.*, "The dynamic window approach to collision avoidance," *IEEE Robotics & Automation Magazine*, vol. 4, no. 1, pp. 23–33, 1997.

[4] M. Svenstrup, T. Bak, and H. J. Andersen, "Trajectory planning for robots in dynamic human environments," in *Intelligent Robots and Systems (IROS), 2010 IEEE/RSJ International Conference on*, pp. 4293–4298, IEEE, 2010.

[5] E. T. Hall, R. L. Birdwhistell, B. Bock, P. Bohannan, A. R. Diebold Jr, M. Durbin, M. S. Edmonson, J. Fischer, D. Hymes, S. T. Kimball, *et al.*, "Proxemics [and comments and replies]," *Current anthropology*, pp. 83–108, 1968.

[6] M.-L. Barnaud, N. Morgado, R. Palluel-Germain, J. Diard, and A. Spalanzani, "Proxemics models for human-aware navigation in robotics: Grounding interaction and personal space models in experimental data from psychology," in *Proceedings of the 3rd IROS2014 workshop Assistance and Service Robotics in a Human Environment*, 2014.

[7] A. Cosgun, D. Florencio, H. I. Christensen, *et al.*, "Autonomous person following for telepresence robots," in *Robotics and Automation (ICRA), 2013 IEEE International Conference on*, pp. 4335–4342, IEEE, 2013.

[8] S. Thrun, W. Burgard, and D. Fox, *Probabilistic robotics*. MIT press, 2005.

[9] M. Bennewitz, W. Burgard, G. Cielniak, and S. Thrun, "Learning motion patterns of people for compliant robot motion," *The International Journal of Robotics Research*, vol. 24, no. 1, pp. 31–48, 2005.

[10] C. Fulgenzi, C. Tay, A. Spalanzani, and C. Laugier, "Probabilistic navigation in dynamic environment using rapidly-exploring random trees and gaussian processes," in *Intelligent Robots and Systems, 2008. IROS 2008. IEEE/RSJ International Conference on*, pp. 1056–1062, IEEE, 2008.

[11] A. F. Foka and P. E. Trahanias, "Probabilistic autonomous robot navigation in dynamic environments with human motion prediction," *International Journal of Social Robotics*, vol. 2, no. 1, pp. 79–94, 2010.